SANDIA REPORT
SAND2007-7456
Unlimited Release
Printed November 2007

Ultrafast NanoLaser Device for Detecting Cancer in a Single Live Cell

Paul L. Gourley, Anthony McDonald

Prepared by
Sandia National Laboratories
Albuquerque, New Mexico 87185 and Livermore, California 94550

Sandia is a multiprogram laboratory operated by Sandia Corporation,
a Lockheed Martin Company, for the United States Department of Energy's
National Nuclear Security Administration under Contract DE-AC04-94AL85000.

Issued by Sandia National Laboratories, operated for the United States Department of Energy by Sandia Corporation.

Available to DOE and DOE contractors from
U.S. Department of Energy
Office of Scientific and Technical Information
P.O. Box 62
Oak Ridge, TN 37831

Telephone: (865) 576-8401
Facsimile: (865) 576-5728
E-Mail: reports@adonis.osti.gov
Online ordering: http://www.osti.gov/bridge

Available to the public from
U.S. Department of Commerce
National Technical Information Service
5285 Port Royal Rd.
Springfield, VA 22161

Telephone: (800) 553-6847
Facsimile: (703) 605-6900
E-Mail: orders@ntis.fedworld.gov
Online order: http://www.ntis.gov/help/ordermethods.asp?loc=7-4-0#online

Table of Contents

Ultrafast NanoLaser Device for Detecting Cancer in a Single Live Cell

PI: Paul Gourley 8331

Introduction

Emerging BioMicroNanotechnologies have the potential to provide accurate, realtime, high throughput screening of live tumor cells without invasive chemical reagents when coupled with ultrafast laser methods. These optically based methods are critical to advancing early detection, diagnosis, and treatment of disease. The first year goals of this project are to develop a laser-based imaging system integrated with an in- vitro, live-cell, micro-culture to study mammalian cells under controlled conditions. In the second year, the system will be used to elucidate the morphology and distribution of mitochondria in the normal cell respiration state and in the disease state for normal and disease states of the cell. In this work we designed and built an in-vitro, live-cell culture microsystem to study mammalian cells under controlled conditions of pH, temp, CO_2, Ox, humidity, on engineered material surfaces. We demonstrated viability of cell culture in the microsystem by showing that cells retain healthy growth rates, exhibit normal morphology, and grow to confluence without blebbing or other adverse influences of the material surfaces. We also demonstrated the feasibility of integrating the culture microsystem with laser-imaging and performed nanolaser flow spectrocytometry to carry out analysis of the cells isolated mitochondria.

Culture Systems Materials and Cavity Design

A motivating factor in this work was to overcome several technical problems with imaging in conventional culture flasks. These flasks are formed with Injection molded plastics and are convenient for cell culture, but present severe limitations for high quality optical imaging. Imaging is limited to reflectance mode through a polystyrene wall of thickness 0.7 mm, since transmittance would occur through 2 walls along with fluid media (~ 5 mm) and air space (~1 cm) and effects of condensation on the upper flask window. The range of transmission of light through polystyrene is limited by the absorption onset near 340 nm. Stress birefringence is a problem when using polarized light. Thermal differential index of refraction is about 10 time larger than that of glasses. The refractive index of polystyrene in the visible is about 1.59 and is not matched to the glass, to the oil immersion lens, or to the oil. Further, the Abbe number of polystyrene is 30 compared to glass values near 55, resulting in high dispersion. Thus, a microculture comprising high quality optical surfaces is imperative for better images.

We also sought to eliminate technical problems with imaging under microscope coverslips on slides. Microscopy of live cells in coverslip/microslide cavities is hindered by cell blebbing (formation of membrane vesicles to maintain homeostasis with environmental changes) and in extreme cases, cell apoptosis. In initial experiments, we showed that it is possible to microfabricate sealed cell microchamber plates to minimize

these effects to slow the formation of blebs and apoptosis by a factor of about 10, to the point where cells retain good morphology and were able to attach to the slide surface. These data show that live cells can be imaged in simple microfabricated cavities for short periods of time (few hours) without more complicated thermo-regulation of culture.

However, we concluded that optimum results require a more sophisticated system for thermoregulation for maintaining cell viability over extended (>2 hours) periods of time. Consequently, a live cell culture microsystem with closed and open perfusion was implemented on a Zeiss Laser scanning confocal microscope platform. This microculture system was developed using a modified version of the LaCon cell culture system for microscopy. This system allows improved optical access and use of the best oil immersion microscope objectives to allow a full range of optical techniques and higher standards of microscopic analysis of living cells. In addition, heated microscope stages and climate boxes were employed to allow observation of cells under stabilized temperature.

The microculture chamber is mounted on a heating frame which can be inserted into a translation stage on the microscope. Cells could be cultivated on glass or a gas permeable foil. The chamber has the advantages of being easy to use, rapid to assemble, uses non-toxic materials, and all parts can be sterilized. The chamber is illustrated in Fig. 1 and employs a base plate of anodized aluminum with stainless steel screw rings holding 0.17 mm cover slips of borosilicate glass held apart by a thin silicone gasket of thickness 0.7 mm. The borosilicate glass is preferred for index matching to the oil and objection lens. As an alternative, quartz may also be used and has the advantage of being easily plasma-etched for microfabrication purposes. We were also able to deposit thin optical or polymer films to modify the properties of the glass surfaces to enhance optical contrast or aid biocompatibility. The geometry of the cell culture is a thin 0.7 mm disk with 32 mm diameter. The culture volume is about 500 ul, about 100 times smaller than the traditional culture flask volume.

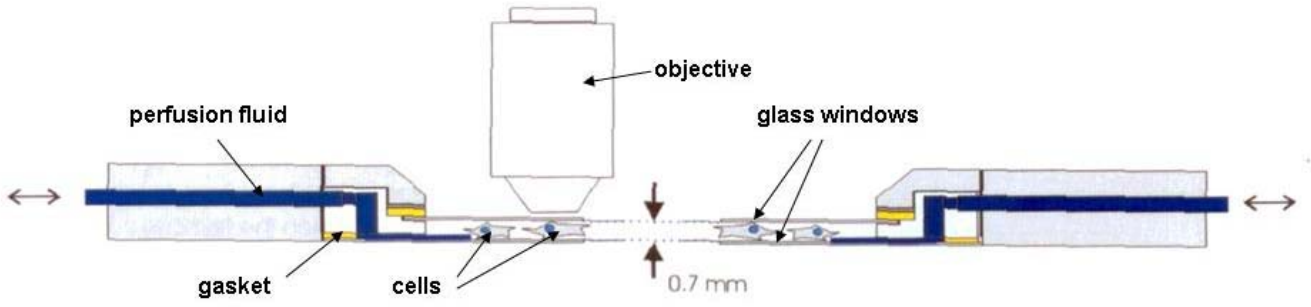

Fig. 1. Cross sectional view of the microculture system showing perfusion fluid lines (blue), silicon gaskets (yellow), and metal housing with borosilicate glass windows.

The micro system could be operated in a closed or open mode (culture open to ambient air via a thin foil cover) in a climate box capable of holding the correct temperature (37 C) and the pH-value of the medium in which the cells are being cultured by regulation of the CO_2. This is an important step in stabilizing specific parameters for the standardization of in vitro tests. In the closed microculture mode, the culture was perfused (i.e. a liquid was pumped through the culture to bathe it with nutritional media or to perform chemical processes to remove cells from surface or to attach fluorescent molecular dyes to label the cell components)

Assembly and Operation of the Perfusion Chamber

The perfusion chamber was assembled into the unit shown in Fig. 1 after autoclaving (sterilizing) all of the components. The aluminum black anodized 58x5.5 mm base plate was placed onto a sterile surface and overlaid with a 42 mm glass cover slip. Next, a 42 mm x 2 mm x 0.5 mm silicon gasket was placed onto the cover slip. A perfusion stainless steel adapter ring was inserted over the silicon gasket, followed by a top 32 mm cover slip and then a 32 mm x 0.1 mm silicon gasket. Finally, a stainless steel screw ring was inserted into the adapter and the assembled system was tightened with a key tool. After assembly, we attached sterilized tygon tubing over the inlet and outlet canal ports in the perfusion adapter. To ensure sterility, the assembled chamber could be autoclaved again. In the last step, the cells were carefully injected into the micro chamber using sterilized pipettes or a mechanical pump. Care was taken to avoid air bubbles.

We employed 3 types of perfusion, full flush, continuous, and microinjection. The full flush employed several microliters of fluid (several times the volume of the microchamber) to completely flush out existing fluid or pre-wet an assembled dry cavity. This single-shot perfusion occurred in a few seconds and was useful for exchanging fresh media for polluted media used after hours of culture growth. Continuous perfusion was performed with a small mechanical pump to slowly and constantly pass a fresh culture medium cocktail from a reservoir tube through tygon tubing through the microchamber and into a waste tube. The perfusion speed can be varied, but an optimal flow rate for a cell culture occurred between 0.1 and 0.25 ml/hour. Microinjection of molecular probe dyes or chemical reagents was performed by manually injecting a small (~ 1 microliter) volume through a very short tube into the chamber. During perfusion, special care was taken to orient the chamber and maintain tubes horizontal in the plane of the chamber to avoid gravitational effects.

Both medium scale (10 ml) and microscale (500 ul) culture systems were implemented to compare cell growth on the two scales. Also, the implementation of successful tissue culturing on the microscale requires methods for sterilizing microcomponents and developing means for manipulating the much smaller cell environment using perfusion techniques rather that the traditional cell culture method of large flasks with permeable membrane gas exchange.

Autoclaving micro components and aseptic technique

Since microorganisms are ubiquitous on the surface of all objects, in the air, and nearly everywhere in the environment, aseptic (sterile) techniques are required to minimize contaminating organisms in the microculture. A majority of the problems in tissue culture work can be eliminated by good sterile techniques. Thus, a conscious and concerted effort was made to keep microorganisms out of the sterile environment. To eliminate contaminants like bacteria, we set up a 2340EA Tuttnauer autoclave system. We operated the system at a temperature of 121 degrees C for 30 minutes with a drying time of 1 hour. Because of the smaller dimensions, autoclaving of micro components is more demanding than larger plasticware or metal parts. To ensure better sterilization, we preloaded the micro component surfaces (orifices, holes, inner spaces, inner tube spaces, etc) with water. This had the effect of internal generation of pressurized steam evolved in those small spaces and resulted in good thermal contact. As a rapid alternative to autoclaving, we also used ethanol sterilization for some components that were less critical to performance.

Tissue Culture Seeding

The majority of our tissue cultures were obtained from American Type Culture Collection (ATCC) in a 1 ml vial/ampule with culture medium comprised of Dulbecco's modified Eagle's medium (DMEM) with a 4.5 g/L glucose, 90%; fetal bovine serum, 10% cocktail. The function of the cocktail was to provide nutrients for the tissue cultures. In addition, the freeze medium in which the tissue culture was stored comprised culture medium, 95%; dimethylsulfoxide (DMSO), 5%. The cells were received in a container of dry ice of which we then placed within a dewar of liquid nitrogen until seeding the cells. Seeding the specific cell line of interest required thawing by rapid agitation in a 37 degree Centigrade water bath. After melting it was immersed in 70% ethanol at room temperature, to inhibit the growth of any bacterial microorganisms during transfer to a test tube or flask. We transferred the cell suspension into a culture flask that contained approximately 10 ml of the culture medium cocktail and then incubated at 37 C with 10% CO_2 in air atmosphere. It was important to avoid excessive alkalinity of the medium during recovery of the cells, so the pH was adjusted, as necessary, prior to the addition of the ampule contents. The bicarbonate content of the culture medium determined whether an atmosphere containing CO_2 was required.

Culture growth observations

Before imaging cells in a culture, the culture's general health was assessed to see if the medium was discolored or appeared milky or cloudy. A cloudy appearance indicated that culture had become contaminated with bacterial microorganisms. The pH of the culture medium was gauged by observing the color of the indicator, phenol red. As a culture becomes more acidic, the indicator shifts from red to yellow. As the culture becomes more alkaline, the color shifts from red to fuschia. As a generalization, cells can tolerate slight acidity better than they can tolerate shifts in pH above pH 7.6. The pH of fresh media was about 8.2 and old media in culture about 7.5.

Using a microscope at low power, we determined if the majority of the cells were well attached and spread out or if the cells were floating in the culture medium. Most of the experiments showed that the cells were well-adhered to the microplate surfaces. We also estimated the confluency percentage by comparing the amount of space covered by the cells with the unoccupied spaces. We also paid special attention to the cell shape as a guide. We noted that round cells in an un-crowded culture was not a good sign unless the cells happen to be dividing cells. We could also observe doublets or dividing cells. Generally we did not observe many giant cells that occur as the tissue culture ages or declines in "well-being". In our initial experiments we limited the growth time to less than 2 days. We observed that a successful "culture seeding " was the rate at which the cells in the newly established cultures attach and spread out. Attachment within an hour or two suggested that the cells had not been traumatized. We also observed that transformed cells, due to a lack of contact inhibition, tended to "pile up" when the culture became crowded (confluent).

Laser Scanning Imaging of Cells

The micro culture system is useful for a variety of cell types and we initially examined yeast and mouse liver cells. Most of the experiments reported here were performed with Mouse liver normal and transformed cells (ATCC# TIB-73, and TIB-76, respectively). TIB-73 is a normal liver cell and TIB-76 is the chemically-transformed version of the mouse liver cell line derived from the normal BALB/c embryonic liver line. This line was transformed with nitrosoguanidine and cloned in agar. These cells grow in 0.3% agarose and produce tumors in both normal syngeneic mice and immunodeficient ATxFL mice.

The initial experiments assessed the ability to grow viable cell culture (TIB-73 and TIB-76 liver cells) in the closed perfusion system compared to the cultures grown by the traditional flask method that we have employed for several years. After seeding of the perfusion chamber from the 50 ml volume flask, we discovered that the cells indeed did adhere to the perfusion cover slips and maintained viability for more than 50 hours.

To assess overall health of the cells in microculture, we developed a rapid imaging technique dubbed "Shadow Phase Contrast" using eccentric annular illumination or light collection. The method can be used with either broadband light for viewing by eye or monochromatic light for laser scanning. This method provides very high contrast and renders images with 3 dimensional qualities. The contrast is wavelength dependent and offers the possibility of inferring chemical information from cells without using molecular probes. Fig. 2 shows a shadow phase contrast image of a TIB76 cell taken about 15 hours after seeding onto the glass surface in the micro culture system. The cells exhibit good adherence properties and show signs of healthy growth by well-formed intracellular organelles, nucleus, mitochondrial reticulum, and nuclear chromatin.

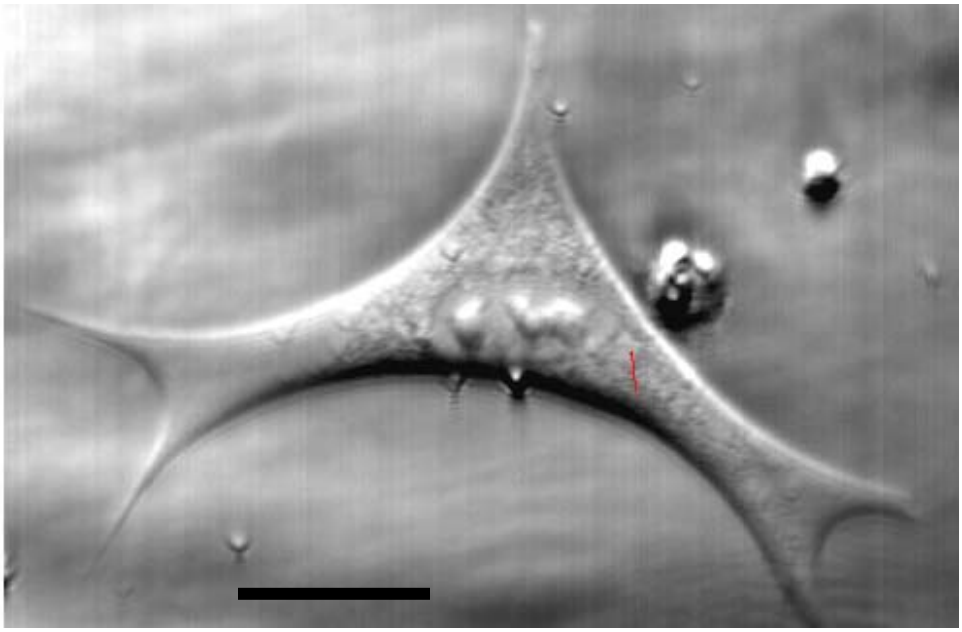

Fig. 2. Laser scanning phase contrast image of TIB76 cell in microculture system. 10 μm scale bar

Additional imaging modalities, including native fluorescence and mitotracker molecular probes were employed to determine the health of the adherent cells. These images are shown in Fig. 3. The upper left image in Fig. 3 is recorded with shadow phase contrast (grey scale) and native fluorescence under laser irradiance at 514 nm. Image B shows that very high contrast details can be observed in the nucleus (condensed chromatin) and in the cytoplasm (peroxisomes). The adherent cells show more internal cell structure than cell suspensions placed under coverslips on microslides. The reason is that suspended cells are more 3 dimensional, spherical and are more difficult to see through. In distinction, the adherent cells are very thin (1-3 microns), more spread out, and 2 dimensional. This more planar geometry facilitates optical access to the internal cell structure. This is a significant advantage for imaging live cells in microculture.

Fig. 3 A shows the native fluorescence from the cell excited at 514 nm (weak yellow). This excitation wavelength was chosen because it is near a sharp absorption peak in the cytochrome a spectrum shown in Fig 4C. Cytochrome a occurs in the mitochondria and it was of interest to see if significant native fluorescence could be observed there. Another source of native fluorescence is flavin adenine dinucleotide (FAD). Upon bonding to two hydrogen atoms, FAD reduction is used by organisms to carry out energy requiring processes. FAD, and the more common Nicotinamide adenine dinucleotide (NAD) is reduced to NADH in the citric acid cycle during aerobic respiration. These molecules serve as reducing agents in several biochemical

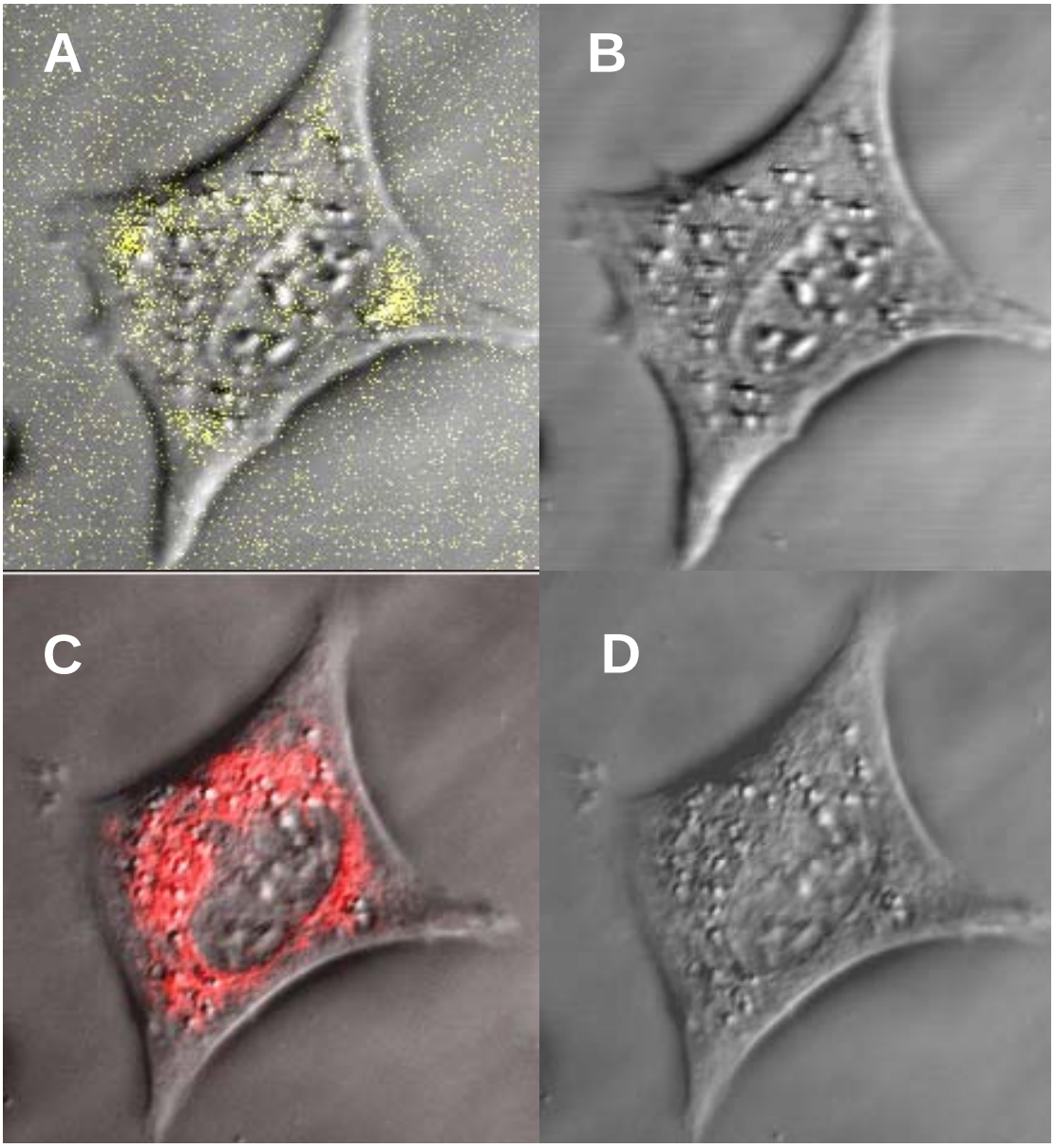

Fig. 3. Laser scanning confocal phase contrast images recorded at 514nm (A and B) and 633 nm (C and D). Native fluorescence is superposed in A and mitotracker red fluorescence is superposed in C. (10 um bar in D).

processes of the cell. FAD absorbs in the same spectral range as cytochrome and has a high fluorescent efficiency shown in Fig 4B. The image A in Fig. 3 shows that a weak native fluorescence occurs away from the nucleus and near the 4 psuedopodia that attach to the glass surface. Since the mitochondria occur near the nucleus this suggests that fluorescence is not associated with cytochrome a, but probably FAD.

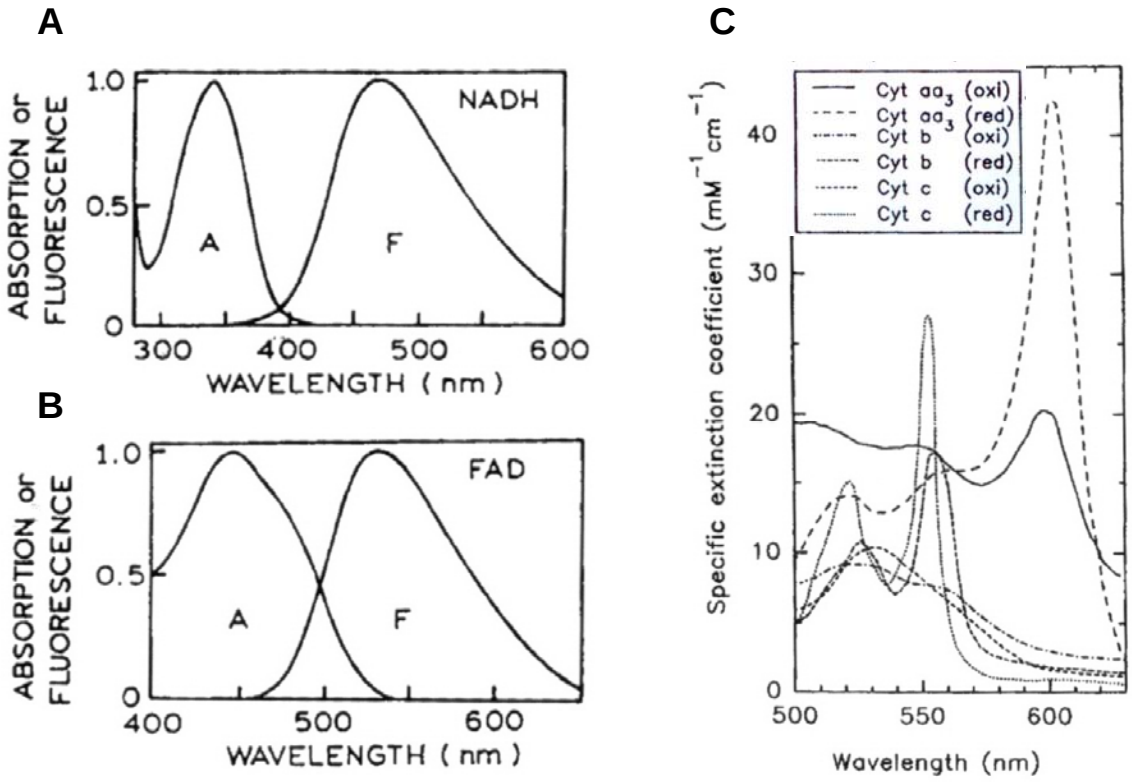

Fig. 4. Absorption and fluorescence spectra of (A) NADH and (B) FAD. (C) Absorpton spectra of cytochromes. (adapted from Lackowicz).

Images of the same cell were recorded after microinjection of the culture media with a small amount of mitotracker red probe. The probe attaches to mitochondria to identify their location in the cell. The probe was excited at 633 nm and emits near 680 nm. It was observed that the microinjection immediately (within seconds) labeled the mitochondria. The perfusion labeling was fast-acting, very efficient, and represents a huge advantage over conventional labeling of suspended cells (requiring incubation for 20 minutes, spinning, rinsing and resuspending cells).

At the same time, phase contrast images were obtained at 633 nm. The resulting phase contrast images with and without mitotracker fluorescence are shown in Fig. 3C and D, respectively. Image D shows that the phase contrast is lower at 633 nm than it is at 514 nm in image B. This indicates a significant decrease in refractive index with increasing wavelength. Note also that the contrast changes are differential, i.e. the nucleus components changed more that the cytoplasmic components. This indicates that phase contrast has the potential to measure biomolecular composition in the cell.

The mitochondria occur as filamentous networks near the cell center in Fig. 3C and were observed to move with time. This is indicative of a healthy respiring cell adapting to varying energy demands during cell growth. Also, little background fluorescence was observed, and no special flushing of unbound dye was required. This is another advantage that occurs because of the thin confining dimension of the culture. A detail of the mitochondrial network is shown in Fig. 5. This image was taken with mitotracker

red fluorescence (red) and ultra-dark field light scattering (white areas), simultaneously. In previous experiments with suspended cells, we observed a strong correlation between the red and white signals. In that case, the mitochondria exist more often in spherical form with diameters near in the range D = 650 to 700 nm. In the present case with strings, the correlation is still observed, though the light scattering is weaker from the much thinner (d~ 400 nm diameter) strings. From classical light scattering, we expect a dependence $(D/d)^4$ ~ 16 times decrease in total scatter for strings versus spheres. The upper image in Fig. 5 shows strong light scattering from the tip of the string, but not detected from the string itself. This suggests that the membrane surface tension creates a balled tip to increase the diameter of the string end.

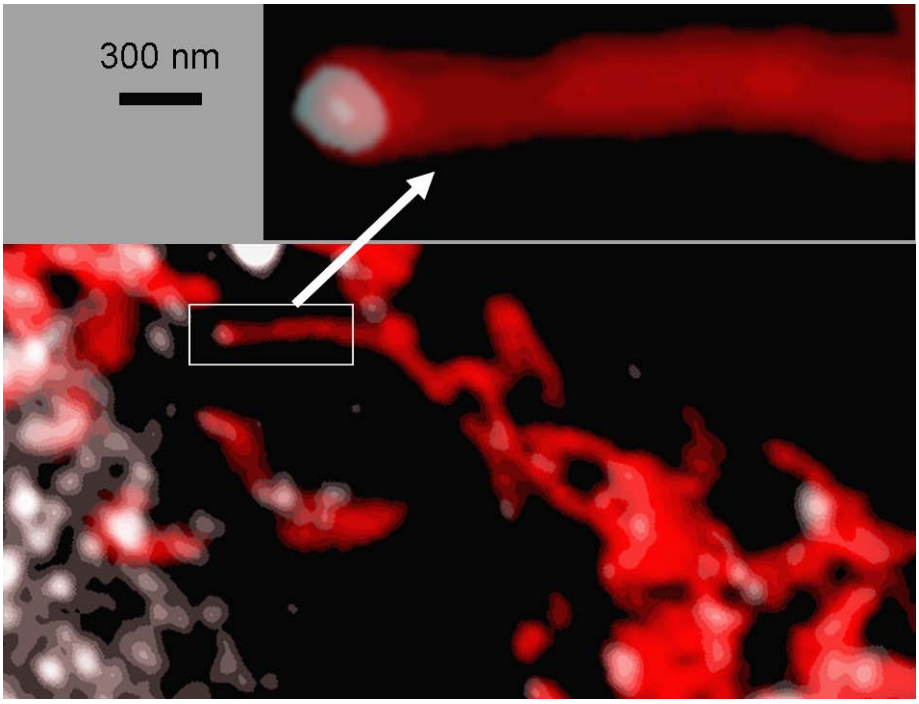

Fig. 5. Mitotracker red fluorescence from the mitochondrial network in a cell. A detail of a the string-like morphology of the respiring mitochondria is shown at high magnification in the upper image.

Observations of cells after 2 days in microculture

We performed an extended time growth to monitor the cell viability. We purposely limited the culture to only one manual full flush perfusion with fresh media at 24 hours to subject the cells to worst case conditions to induce grossly observable changes. After 48 hours with only one perfusion, we noticed that the culture medium had some bacteria, the cells morphology degraded and some cells detached from the surface. We expect that the bacteria came from lack of initial sterility of the surfaces. The other factors result from the small volume of the culture and attendant build up of metabolic

waste products, changes in pH (measured increased from 8.5 initially to 7.2), alteration in CO_2 or inadequate perfusion (a different medium was used other than the cocktail). The culture medium that was used initially had no fetal bovine serum added to the DMEM, which is a protein that is vital to cell viability. Also when we added a molecular probe to the culture, we could have introduced adverse effects that changed the biological environment of the cell culture medium. Despite these worst case conditions, it was still possible to image viable cells after ~50 hours of culture suggesting that microculture had successfully met its performance goals. In the second year, we will perform more rigorous testing under more ideal condtions to determine the long term growth limits of microculture.

Microscopic comparison of adherent and suspended cells

We have set up both macro- and micro- culture systems for cancer cell experiments and have cultured a number of cell lines including liver and yeast cells and demonstrated the viability of the systems to grow cells. We have performed live cell imaging on both adherent cells and cells in suspension using a variety of laser microscopy techniques including fluorescence, ultra-dark field, and high phase constrast. Some of these images are shown in Fig. 6 and 7 which are overlaid images of fluorescence and light scattering images. We discovered phenomenonal changes in light scattering intensity (several orders of magnitude!) as the mitochondria underwent fragmentation when the adherent cells were removed from culture surface by trypsin. Normally the mitochondria exist in a reticulum with threads of diameter d ~ 200nm in diameter as shown in Fig 6A and 7A. This diameter is in the Rayleigh light scatter regime so that the mitochondrial scatter is relatively small compared to other larger organelles in the cell (peroxisomes). Those other organelles dominate the light scatter from adherent cells which has a flat 2D geometry. With trypsinization and resulting mitochondrial fragmentation, the mitochondria changed from thread to spherical fragments with diameter d ~700 nm as shown in Fig. 6C and 7C. Light scattering by these larger diameter mitochondria occurs in the Mie scattering regime where the light scattering intensity I ~ d to the 4th power. This 3.5x increase in diameter results ~600x increase in the light scatter. As a result these large changes enabled us to observe striking differences in the mitochondrial morphology of normal and cancer cell types in suspension. Further, these changes in morphology also enabled us to distinguish the disease and normal states in a statistically large ensemble of cells by nanolaser spectroscopy.

In the normal suspended cells, generally the fluorescence is very bright and texture is grainy, with large fluctuations in intensity. In the ultra dark field images, the light scattering occurs predominantly from the mitochondrial network and exhibits strong correlation with the fluorescence images. This correlation is quantified in the cell colocalization histogram (Fig. 6A). It exhibits a very large range of variation of fluorescence intensities corresponding to the mitochondrial signals. Enhancement of light intensity by collective effects may be responsible for this large range in variation. A small percentage (less than 1%) of scattering occurs from other internal organelles. Significant scatter (about 10%) occurs from the cell membrane that is uncorrelated with

mitochondrial fluorescence. The shape of the cell rendered by membrane scatter is often irregular, not round. Additionally there is a small fraction (less than 0.5%) of light

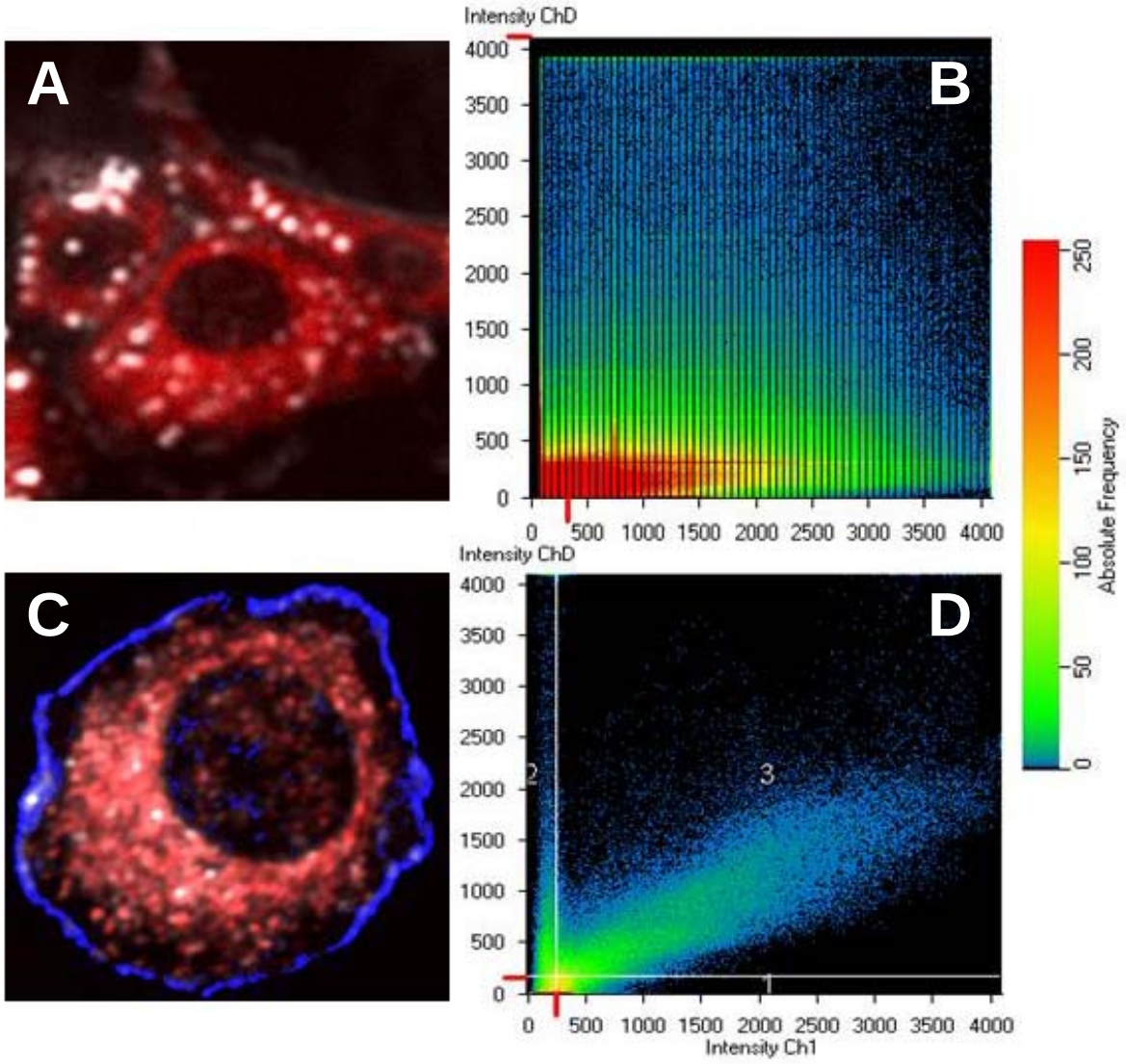

Fig. 6. A. Dual overlay image with Mitotracker red fluorescence and light scattering from Normal (A) adherent and (C) suspended liver cells. (B) and (D) are the corresponding colocalization plots with scattered light (y axis) plotted against fluorescent intensity (x axis).

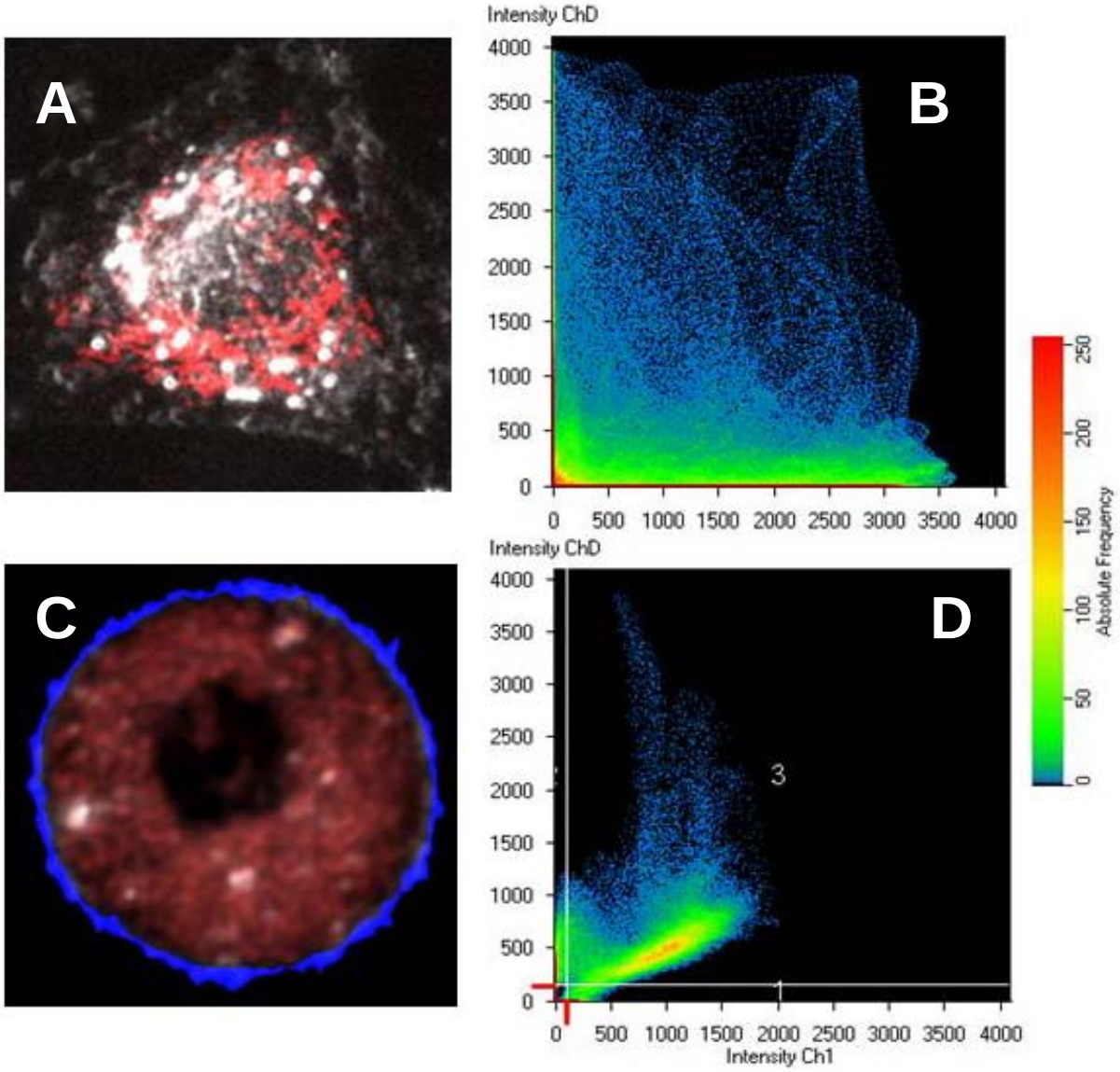

Fig. 7. A. Dual overlay image with Mitotracker red fluorescence and light scattering from Cancer (A) adherent and (C) suspended liver cells. (B) and (D) are the corresponding colocalization plots with scattered light (y axis) plotted against fluorescent intensity (x axis).

scattering from the nuclear membrane that is also uncorrelated with the mitochondrial fluorescence. In sharp contrast to the normal cells, the mitochondria in the transformed liver cells have a very chaotic, unorganized, and random distribution about the cytosol of the cancer cells (Fig. 7C). The fluorescence is uniformly distributed throughout the cytosol and is dull in appearance, much less intense than that in normal cells. The outline of the nucleus, defined by the fluorescence, is more irregular in shape and frequently less ovoid. The light scattering and fluorescence are much lower and exhibit low variance. In contrast to the normal cells, the cancer cells have a very monodisperse distribution as shown in the colocalization histogram (Fig. 7D).

Spatial correlation effects on light scattering in cells

The light scattering from the mitochondrial network in the cells can be analyzed by many-body scattering methods adopted from polymer physics. This analysis enables us to connect the scattering properties to the lasing linewidth measured in experiments. At the heart of this analysis is the light scattering structure factor which plays an important role and is intimately related to cell bioenergetics or thermodynamic quantities. If the scatterers are not identical in their scattering properties, but are identical in their correlation properties, then it is necessary to take account of so-called incoherent scattering. In general, the differential scattering cross section is

$$\partial\sigma/\partial\boldsymbol{\Omega} = S(q)I_c + I_i \qquad (1)$$

The first term in this formula involves the structure factor and the mean scattering amplitude; it is the coherent scattering I_c. The second term comes from the mean square of fluctuations from this mean amplitude. These fluctuations are not correlated at different sites and thus the contributions from each site may simply be added. This contribution is usually known as the incoherent scattering I_i , because correlations play no role. The structure factor is given by

$$S(\mathbf{q}) = 1 + \langle\rho\rangle \int d\mathbf{r}\, exp(i\mathbf{q}\cdot\mathbf{r})[g(\mathbf{r})-1] \qquad (2)$$

where **q** is the change in momemtum of the incident and scattered photon, <p> is the average particle density, and g(r) is the correlation function, describing the fluctuation of the particle density from the mean value. More exactly, the correlation function is related to the correlation integral of the particle density

Fig. 7. A. Dual overlay image with Mitotracker red fluorescence and light scattering from Cancer (A) adherent and (C) suspended liver cells. (B) and (D) are the corresponding colocalization plots with scattered light (y axis) plotted against fluorescent intensity (x axis).

$$\langle\rho(\mathbf{r}')\rho(\mathbf{r}'+\mathbf{r})\rangle = \langle\rho\rangle\,\delta(\mathbf{r}) + \langle\rho\rangle^2 g(\mathbf{r}) \qquad (3)$$

where δ(r) is the Kronecker delta function. The correlation function mirrors the symmetry of the particle distribution, i.e. it is periodic, self similar or random. For a

random distribution, g = 1, so S =1, which is the incoherent scattering condition where phase is random and scattering intensity is simply the incoherent sum of intensities of all individual scatterers. For a periodic distribution or particles, g is periodic, and S is peaked at periodic values of the transfer momentum ***q***. For a self-similar distribution, S is likewise self-similar, comprising features on successive scales of ***q***. For a mesh of

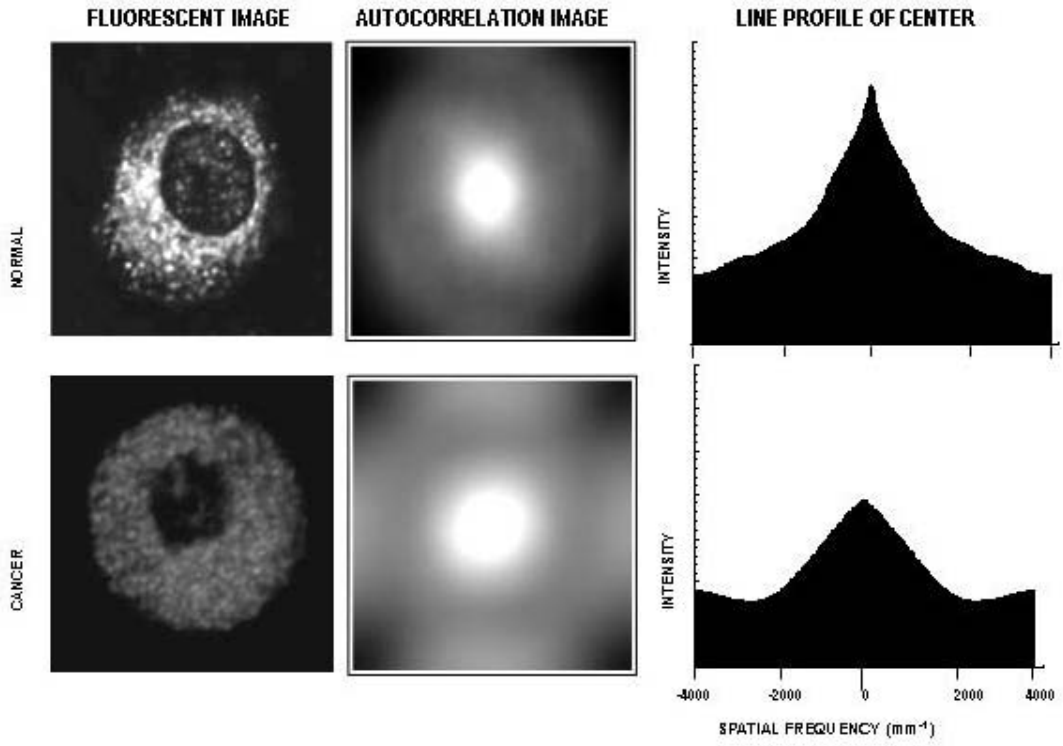

Fig. 8. The difference between a normal and cancer liver cell is shown clearly by the location of mitochondria. The healthy cell shows very few mitochondria near the outer cell membrane; instead they cluster densely as they approach the cell's nucleus (rendered as the black central hole). In the abnormal cell, the mitochondria are spread throughout the cell, do not cluster, and under the same lighting produce a more subdued and uniform image. The correlation image and its line profile reveals the higher spatial correlation of the mitochondria in the normal cell.

interconnected mitochondria, we expect to see scattering features at large angles that reflect the size and shape of the individual mitochonria, and superposed features at smaller angles that reflect the morphology of the mesh or network. The measured 2D spatial correlation functions for the cells are shown in Fig. 8, revealing about 60% higher correlation for the normal cells.

Ultimately, we are interested in the relationship of the mitochondrial morphology on the lasing properties of cells in a biocavity laser, particularly the properties of the lasing spectral data presented in the next section. By integrating Eq. 1 we obtain the total scattering cross section σ_T. For a laser microcavity of length L loaded with scattering centers having average density ρ, the lasing linewidth $\delta\lambda$ in the high scatter limit is given by

$$\delta\lambda \approx (2/\pi)\,(K/P)\,(\rho L\,\sigma_T)^2 \qquad (4)$$

where K is a linewidth enhancement factor, and P is the photon emission rate. Thus, the laser linewidth is sensitive to the scattering of light by mitochondria by a second order dependence on the scattering cross section. Increased scattering by correlation of mitochondria will be evident by broadened lasing linewidth.

Biocavity laser spectroscopy of isolated mitochondria and normal and cancer cells

Previous experiments have shown how dysfunctional mitochondria have been observed to lose network structure, become spherical or swell, lose functionality, and generally lose structural correlation with other parts of the cell. In previous experiments with suspensions of isolated mitochondria we have used biocavity laser spectroscopy to show how mitochondrial swelling results in increased diameter, decreased molecular (protein) concentration, and decreased optical density by at least a factor of two. These changes, illustrated by the shift in biocavity laser wavelength in the inset of Fig. 3, indicate that abnormal mitochondrial would exhibit a decrease in optical scattering just as observed in the imaging data above. Thus, mitochondria in compromised cells would exhibit less turbidity, less scatter, and be more uniform in appearance as observed in these images. These observations suggest that mitochondria scatter in a biocavity laser may serve as useful markers for detecting disease without use of molecular probes or other reagents that require more time for specimen preparation.

In separate experiments, suspensions of normal and transformed liver cells were studied by biocavity laser spectroscopy. The cells were removed from culture and suspended in buffer solution for flowing through the laser cavity. This technique is the fastest demonstrated method for characterizing a cell in near physiologic condition without staining, requiring only microseconds per cell to acquire information about cell morphology and biochemistry. The benefit of such ultrafast laser techniques has been proposed for realizing pathology of tumors in realtime during surgery.

Cluster plots of spectral parameters showing the measured wavelength shift, peak lasing intensity, and lasing linewidth are shown in Fig. 9. These data reveal a distinct clustering of the cell parameters in two of the three cluster planes associated with lasing wavelength (x axis) and lasing linewidth (y axis). Significantly, the cancer cells have reduced linewidth as expected from mitochondria that exhibit less correlation and less scattering of intracavity coherent light. This is consistent with the observations of less scatter from cancer cells (Fig. 7) compared to normal cells (Fig. 6). The correlated mitochondria in the normal cells result in lasing linewidth that is broader by a factor of about 2. The variance in the linewidths for each type of cell is less than the difference of the mean values, allowing the cell types to be distinguished on the basis of linewidth. At the same time, the wavelength shift (proportion to total cell optical density) is about 50% larger for the normal cells compared to the cancer cells. The observation of less optical density for cancer vs normal has also been observed for brain cells (gliobastoma and normal astrocytes).

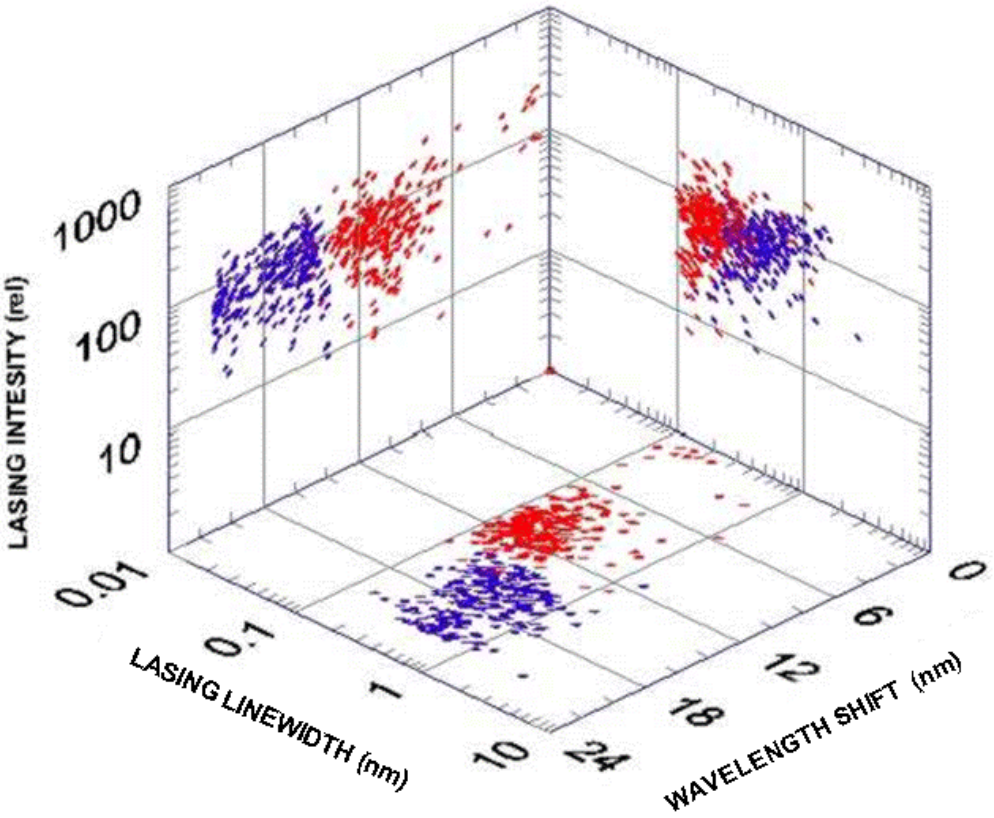

Fig. 9. Cluster plot of spectral parameters showing distinct clusters of points for normal (blue) and transformed (cancer) cells (red).

In a separate set of experiments performed on yeast, we discovered that isolated mitochondria can be studied by nanolaser spectroscopy to assess the optical density of an individual mitochondrion. This measurement uniquely reflects the mitochondrion size and biomolecular composition. As such, the optical density is a powerful parameter that rapidly interrogates the biomolecular state of single cells and mitochondria. Wild-type cells and mitochondria produced Gaussian-like distributions with the optical density converging to a single peak. In contrast, mutant cells and mitochondria produced distributions that were asymmetric, and highly skewed. These distribution changes could be self-consistently modeled with a single, log-normal distribution undergoing a thousand-fold increase in variance of biomolecular composition. These features reflect a new state of stressed or diseased cells that we call a Reactive Biomolecular Divergence (RBD) that reflects the vital interdependence of mitochondria and the nucleus.

We elected to use nanolaser spectroscopy to study isolated mitochondria from the liver cells to examine the possibility of measuring mitochondrial laser shift distributions. To do so we had to extract the mitochondria from the cell in order to observe, to study, and to examine their properties. We used a mechanical technique called “Dounce Homogenization” which isolated the mitochondria. In the extraction process, the mitochondria we observed are fragmented into balls of approximately 500 nanometers in diameter.

Using nanolaser spectroscopy, we performed preliminary measurements of mitochondrial lasing spectra. We were able to determine that the nanolaser spectra are able to reveal the distribution of individual wavelength shifts for the tiny organelles. The distribution of shifts is shown in Fig. 10 for normal mitochondrial and exhibit a peak with a long tail to longer wavelengths. Additional analysis is needed to interpret these and other cancer cell mitochondria data to reach any firm conclusion. But these suggest the intriguing possibility that Nanolaser spectroscopy of isolated mitochondria extracted from cells could form the basis for a general technique that can rapidly quantify the degree of health or disease in human cell types.

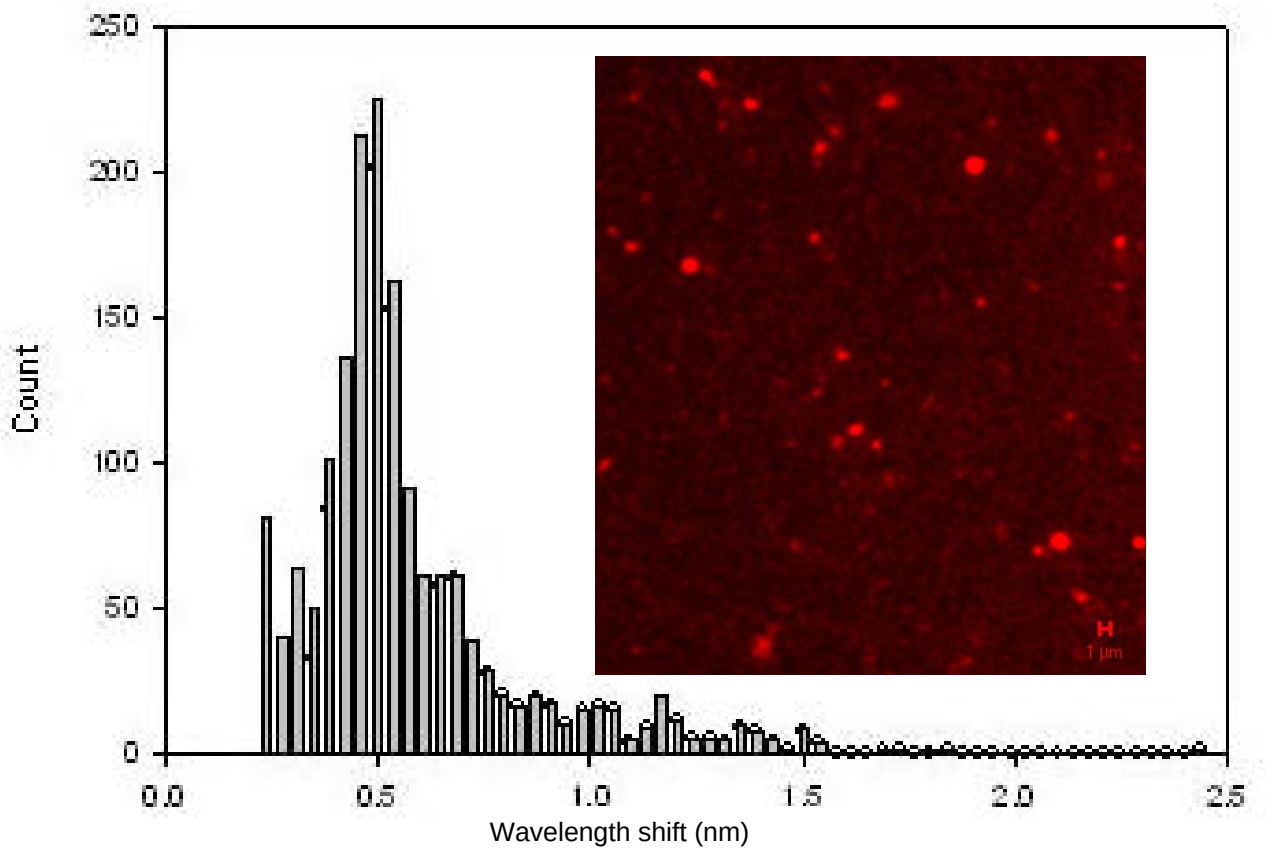

Fig. 11. Laser scanning micrograph and histogram of wavelength shifts for isolated mitochondria from normal liver cells.

Discussion and Summary

We developed a microculture system that was relatively easy to use, performed exceptionally well for growing adherent cell cultures, and permitted new kinds of experiments to be performed. The advantages stem from several enabling features. First, the high quality glass material optics allowed biocompatible surfaces, index matching, surface functional layers and is suitable for micro-etching and deposition of dielectric or conductive layers. Second, the thin imaging cavity formed by the microculture chamber allowed full optical access for all of the imaging modalities of the laser scanning microscope. These include reflectance, transmittance, fluorescence, normal and shadow phase contrast, differential interference contrast, and ultra-darkfield microscopy. Third, high resolution imaging of intracellular structure was possible because of the 2-dimensional nature of the adherent living cells. The images of the cultured cells were more detailed than in previous studies using microscope slides. In particular, the shadow phase contrast technique showed exceptionally sharp, high contrast images of organelles like peroxisomes. And, the string-like morphology of the mitochondria was easily observed and measured with fluorescent probes. Also, the perfusion capability of the small 500 microliter volume chamber worked especially well for maintaining culture conditions, labeling cells during growth, and introducing other molecular species like trypsin or other enzymes or cell stimulants to effect changes in cell adherence or growth. With a large culture flask, this fete is nearly impossible to accomplish.

Mitochondria are dynamic intracellular organelles that play a central role in cell function, oxidative metabolism and apoptosis. The recent resurgence of interest in the study of mitochondria has been fuelled in large part by the recognition that genetic and/or metabolic alterations in this organelle are causative or contributing factors in a variety of human diseases including cancer. Several distinct differences between the mitochondria of normal cells and cancer cells have already been observed at the genetic, molecular and biochemical and biophysical levels. Certain of these alterations in mitochondrial structure and function might prove clinically useful either as markers for the early detection of cancer or as unique molecular sites against which novel and selective chemotherapeutic agents might be targeted. Given the importance of mitochondria in the development of disease such as cancer and respiratory failure, it is crucial to develop methods for detecting changes in mitochondria as a marker for early detection. And, photonic techniques are expected to play a significant role because they have the capacity for ultra high speed detection of large numbers of organelles and cells to permit accurate assessment of the statistical variations in a large population. We developed a mathematical relationship between the mitochondria correlation structure factor and lasing linewidth. Experiments demonstrated that mitochondria dominate the light scatter from cells that are in the suspended state appropriate for flow measurements. The mitochondria are more spatially correlated in normal cells and exhibit stronger scattering of light. Mitochondria are larger, less optically dense, and less correlated in diseased cells. These differences enabled biocavity laser spectra to distinguish between healthy and cancerous conditions in single cells.

Publications

Reactive Biomolecular Divergence in Genetically Altered Yeast Cells and Isolated Mitochondria as Measured by Biocavity Laser Spectroscopy: A Rapid Diagnostic Method for Studying Cellular Responses to Stress and Disease, Paul L. Gourley, Judy K. Hendricks, Anthony E. McDonald, R. Guild Copeland, Michael P. Yaffe, and Robert K. Naviaux, *J. Biomed. Optics*, accepted. May 2007.

Nanolaser Spectroscopy Of Isolated Mitochondria Paul L. Gourley, Judy K. Hendricks, Anthony E. McDonald, R. Guild Copeland, and Robert K. Naviaux, *Mitochondrion*.

Ultrafast NanoLaser Device for Detecting Cancer in a Single Cell, P. L. Gourley, *Sand Document*, Sept. 2006.

Nanolaser Spectroscopy and Image Correlation Microscopy: New Tools for Cancer Research, Gourley, Hendricks, McDonald, Copeland, Yaffe, Naviaux, Singh, *J. Cancer Research and Treatment* , Jan. 2006, invited article, ***cover story***, published.

Nanolaser spectroscopy of Normal and Genetically altered Yeast and Isolated Yeast Mitochondria, Gourley et al. , *Proc. Conf. on Biomed Optics*, San Jose, Jan, 2006, published.

Presentations

1. Nanolaser spectroscopy of Normal and Genetically altered Yeast and Isolated Yeast Mitochondria, Conf. on Biomed Optics, San Jose, Jan, 2006.
2. Mitochondrial Image Correlation and Cancer, P. L. Gourley, Research for Mitochondria and Cancer Workshop, NIH, September 3-4, 2006 Bethesda, MD
3. New Biophontic Tools for Mitochondrial Research, P. L. Gourley, Mitochondria and Medicine Conference, Hyderabad, India, January 21-25, 2007.
4. Nanolaser Spectroscopy of Isolated Mitochondria, P. L. Gourley, American Physics Society, Denver, CO, March 5-9, 2007


Sandia National Laboratories